doi:10.1006/jmbi.2001.4663 available online at http://www.idealibrary.com on IDEAL® *J. Mol. Biol.* (2001) **309**, 671–685

JMB

Selection, Characterization and X-ray Structure of Anti-ampicillin Single-chain Fv Fragments from Phage-displayed Murine Antibody Libraries†

Jörg Burmester[1], Silvia Spinelli[2], Luisa Pugliese[2], Anke Krebber[1] Annemarie Honegger[1], Sabine Jung[1], Bernhard Schimmele[1] Christian Cambillau[2] and Andreas Plückthun[1]*

[1]*Biochemisches Institut der Universität Zürich, Winterthurerstrasse 190 CH-8057 Zürich Switzerland*

[2]*Architecture et Fonction des Macromolécules Biologiques UMR 6098-CNRS 31 Chemin Joseph Aiguier F-13402 Marseille Cedex 20 France*

**Corresponding author*

Single-chain Fv (scFv) antibody libraries were constructed from mice immunized with an ampicillin-bovine serum albumin conjugate. Several antibodies with specificity for intact ampicillin were selected by phage display and characterized. The antibody scFv fragment aL2 binds to intact ampicillin and shows no detectable cross-reactivity with hydrolyzed ampicillin. We determined the X-ray structures of two crystal forms of w.t. aL2, which differ mainly in the side-chain conformation of Trp H109 (according to a new consensus nomenclature Kabat residue number H95) in the extremely short (three residues) CDR H3 and the presence or absence of a well-resolved molecule of 2-methyl-pentane-2,4-diol in the bottom of the binding pocket. Attempts to co-crystallize aL2 with its antigen or to diffuse ampicillin into the wild-type aL2 crystals were unsuccessful, since crystal contacts obstruct the binding pocket. However, a mutant with two point mutations near the N terminus (Gln H6 replaced by Glu and Ala H10 (Kabat H9) replaced by Gly) crystallized in a form compatible with antigen-binding. Although the mutations affect the conformation of framework I, the conformations of the binding pocket of the uncomplexed wild-type aL2 and of the mutant complex were almost identical. The structure explains the specificity of the antibody for intact ampicillin and the degree of cross-reactivity of aL2 with a wide variety of ampicillin analogs. This antibody system will be very useful as a diagnostic reagent for antibiotics use and abuse, as a model for the effect of expression of antibiotic binding molecules in *Escherichia coli*, and for directed evolution towards high antibiotic resistance.

Keywords: immunoglobulin; scFv, ampicillin; framework structure; antibody engineering

†This paper is dedicated to the memory of the late Professor Dieter Riesenberg.

Present addresses: J. Burmester, Mettler-Toledo GmbH, Im Langacher, CH-8606 Greifensee, Switzerland; L. Pugliese, IRCC Institute for Cancer Research, University of Torino Medical School, Strada Provinciale 142, I-10060 Candiolo (Torino), Italy; A. Krebber, Maxygen, 515 Galveston Drive, Redwood City, CA 94036, USA; S. Jung: Bayer AG, Central Research, Biotechnology/Molecular Biology, Build. Q18, D-51368 Leverkusen, Germany.

J. Burmester and S. Spinelli contributed equally to this work.

Abbreviations used: 6-APA, 6-aminopenicillanic acid; BBS, borate-buffered saline; BSA, bovine serum albumin; CDR, complementarity-determining region; DMSO, dimethylsulfoxide; EBSS, Earle's buffered salt solution; ELISA, enzyme-linked immunosorbent assay; EMCS, *N*-[ε-maleimidocaproyloxy] succinimide ester; GMBS, *N*-[γ-maleimidobutyryloxy] succinimide ester; HBS, Hepes-buffered saline; HCDC, high cell-density cultivation; KLH, keyhole limpet hemocyanin; MPD, 2-methyl-pentane-2,4-diol; MPS, 4-maleinimido-propionic acid-*N*-succinimidylester; MRL, maximum residue level; PCR, polymerase chain reaction; PBS, phosphate-buffered saline; PDB, Protein Data Bank; PEG, polyethylene glycol; scFv, single-chain variable fragment of an antibody; TCA, trichloroacetic acid; THF, tetrahydrofuran; V_H, variable domain of antibody heavy chain; V_L, variable domain of antibody light chain.

E-mail address of the corresponding author: plueckthun@biocfebs.unizh.ch

0022-2836/01/020671–15 $35.00/0

Introduction

Antibodies against antibiotics are important as diagnostic reagents, and their expression in bacteria may be used to study how proteins with the ability to interact with antibiotics can influence bacterial growth and how they can serve as starting points for the evolution of antibiotic resistance. As a model system, we chose antibodies directed against β-lactam antibiotics. These antibiotics act in the periplasmic space and block enzymes involved in peptidoglycan cell wall synthesis.[2] Antibody single-chain fragments (scFv) exported into the periplasmic space can fold to their native conformation efficiently in the oxidizing environment of the periplasmic space, while only a subpobpulation of exceptionally stable antibody fragments is fully functional in the cytoplasm. It should therefore be possible, in principle, to use a challenge with a β-lactam antibiotic to select for improved antibody fragments showing better folding yields, higher stability and/or higher affinity. Furthermore, it might be possible to study the emergence of hydrolysis under selective pressure.

With the widespread use of β-lactam antibiotics in medicine and as an additive in stock farming, anti-ampicillin antibodies are potentially of great value as detection reagents. Maximum residue levels (MRLs) have been defined for veterinary drugs in edible products such as bovine milk.[3] In principle, direct detection by a penicillin sensor based on immobilized β-lactamase is possible,[4] but current screening protocols rely on growth inhibition or competition with radiolabeled penicillin to microbial cells. These tests are generally sufficient for detection of residual ampicillin in milk or meat.[5–7] However, for conclusive results these assays have to be confirmed by physicochemical methods such as liquid chromatography, which require laborious extraction steps and are therefore both time-consuming and expensive.[6] Antibodies specific for β-lactam antibiotics could be used directly for selective screening by enzyme immunoassays as well as for immunoaffinity chromatography, to achieve an efficient enrichment of contaminants from milk or meat products prior to further analysis.[7,8] Since MRLs are defined for the veterinary drug itself and not for their metabolites, the appropriate antibody has to be specific for the intact β-lactam ring.

So far, the generation of such antibodies has been difficult. Due to high reactivity of the β-lactam ring with nucleophiles, the immunogen is quickly degraded *in vivo*, leading to the generation of antibodies against hydrolyzed ampicillin and protein adducts. However, poly- and monoclonal antibodies with specificity for intact β-lactam antibiotics have been described.[7,8] For routine use, polyclonal antibodies are disadvantageous, due to their limited availability, and although this problem can be solved by the use of the hybridoma technique, a large number of different monoclonal antibodies usually have to be screened in order to find a suitable candidate.

In contrast, by using selection techniques such as phage-display,[9] ribosome display,[10] bacterial surface display[11] or yeast display[12] from natural,[13,14] semisynthetic[15] or fully synthetic libraries,[16] the appropriate specificity and selectivity (e.g. the closed β-lactam ring) can be selected for directly. Moreover, once the variable region genes have been cloned, the antibody domains can be further engineered in a multitude of ways to produce antibody variants with higher affinity,[17–19] altered antigen specificity,[20,21] or enhanced stability.[22,23] Furthermore, inexpensive microbial production becomes available for recombinant antibody fragments.[24]

Here, we report an immunization strategy eliciting antibodies specific for the intact ampicillin molecule. The re-engineered and optimized phage-display vector pAK100 was used for cloning of functional scFv antibody libraries derived from spleen-cell repertoires of immunized mice.[25] By different selection strategies, several scFv fragments with different binding specificites were isolated and characterized. We were particularly interested in generating antibodies that would predominantly recognize the non-hydrolyzed β-lactam/penicillanic acid moiety of ampicillin and are tolerant towards substitutions at the amino group of ampicillin, as a starting point for a metabolic selection and *in vitro* evolution project. A group of closely related scFvs showed the desired selectivity, as determined by phage ELISA competition with ampicillin analogs and degradation products. One of these, termed aL2, was produced in *Escherichia coli*, purified by affinity chromatography and its crystal structure was determined. While the wild-type protein could not be crystallized with the antigen in the binding pocket, a mutant protein with point mutations† in the residues H6, H7 and H10[1] (Kabat H9) allowed us to determine the structure of the complex. The understanding of the molecular basis of the exclusive specificity of aL2 for intact ampicillin is expected to allow a rational design of mutants with improved or altered binding properties.

Results

Immunization and scFv antibody library construction

Because of the limited stability of ampicillin in aqueous solution, the protocol for immunization of BALB/c mice was adapted accordingly. KLH was not used as carrier protein, since it contains copper, which is known to catalyze the hydrolysis of ampicillin.[26] Instead, ampicillin was coupled to

† For residue numbering, the unified numbering scheme introduced by Honegger & Plückthun[1] was used. In addition, the traditional Kabat numbering is indicated in parentheses. The correspondence of the two numbering schemes is shown in Figure 1.

bovine serum albumin (BSA), and a mixture of three different linker molecules without aromatic groups were chosen in order to increase the probability of generating antibodies recognizing the hapten independent of the linker moiety. Sixteen days after subcutaneous priming with AdjuPrime (Pierce) and ampicillin/BSA, the immune response was boosted by an intrasplenic injection of the ampicillin/BSA conjugate. This procedure can be used when the amount of antigen is limited,[27] and we employed it to induce an immune response for intact ampicillin rather than for hydrolyzed ampicillin, which will be generated over time. Mouse 2 was boosted by a second intrasplenic injection 37 days after priming. In mouse 4, a second intrasplenic boosting was not possible due to severe scarring and, therefore, it received a booster injection into the tail vein at day 50.

The immune response was analyzed by ELISA before and after immunization. Twenty-three days after initial priming, the serum of all immunized mice reacted positive in binding analysis by ELISA with ampicillin coupled to transferrin, but the signal could not be inhibited by 1 mM ampicillin. In contrast, the last analysis of the serum prior to mRNA extraction (43 days after priming for mouse 2, 54 days after priming for mouse 4) resulted in an inhibition of the ELISA signal by 1 mM ampicillin of 20 % (mouse 2) and 65 % (mouse 4), indicating that the chosen immunization strategy indeed led to a subpopulation of antibodies that recognize free ampicillin. The antibody mRNA was amplified by PCR with primers specific for antibody variable region genes as described.[25] The amplified variable domains of mouse 4 were assembled into an scFv library, cloned into the phage display vector pAK100[25] and, after transformation into *E. coli* XL1-Blue cells, 10^7 independent colonies were obtained.

Selection of anti-ampicillin scFvs by phage panning

Phages were panned on transferrin-EMCS-ampicillin and eluted by different methods. Unspecific elution with glycine/HCl (pH 2.2) and competitive elution with ampicillin both enriched the antibody scFv fragment aL2 (Figure 1) after two rounds of phage panning of the antibody library derived from mouse 4.[25] After rounds 2 and 3, ten other positive clones with similar binding properties, as judged by phage-ELISA analysis, were sequenced and all found to be very similar to aL2 (all >95 % sequence identity, Figure 1). Some sequence variation at the N termini of both the L and H chain may have been introduced by the degenerate primers used for cloning (L4, Met, Leu, Ile; H7, Ser or Pro), while the internal variations may have resulted from somatic mutations or from errors introduced by the PCR amplification. aL2 has a kappa light chain, which showed 88 % identity (91 % similarity) with the most closely related murine kappa germline sequence (IGKV6S5) listed in the IMGT database†. The aL2 V_H sequence showed 98% identity/similarity to the closest murine VH germline sequence (VH1 B1c) listed in the ABG database‡.

We investigated whether the variation of elution conditions during several rounds of phage panning would result in enrichment of different antibody sequences from a given library. Therefore, alternative specific elution strategies using different ampicillin analogs were tested to see whether the mouse 4 library contained anti-ampicillin antibodies different from aL2. Competitive elution from the ampicillin-derivatized panning surface with hydrolyzed ampicillin resulted in an enrichment of aL4 and aL5 after two panning rounds. The elution with 6-APA lead to an enrichment of aL5 and aL6 after three panning rounds (Figure 1 and Figure 2(a)). In contrast to aL4 and aL5, aL6 is closely related to aL2 (93 % identity, 95 % similarity in V_L, 85 % identity, 91 % similarity in V_H), but shows a clearly distinct antigen combining site. The exclusive appearance of aL2 on the one hand, and aL5 and aL6 on the other, as a function of the competitor used in phage elution correlates with the inhibition profiles in phage-ELISA analysis. Here, aL5 and aL6 could be inhibited more strongly with 6-APA (data not shown) and aL2 could be inhibited more strongly with ampicillin, which reflects the criteria for enrichment during the phage-panning process. Although the intensity of the non-inhibited ELISA signals is very similar for aL2, aL4 and aL5, the aL2 scFv is strongly enriched by phage elution with glycine/HCl after only two rounds of phage-panning, and demonstrates that aL2 is the most abundant binder in the scFv library. This may be due to its predominant presence in the immune response of the mouse or to its preferential amplification by PCR or phage proliferation.[28] The strategy of specific elution by analogs of the antigen therefore proved to be a very straightforward method for enrichment of antigen-specific antibodies such as aL5 and aL6, which would otherwise not appear after several rounds of phage panning. From the selected antibodies, aL2 was chosen for further characterization, because its unambiguous specificity for free ampicillin.

Purification and characterization of aL2

From a one liter expression culture ($A_{550} = 46$), 30 mg of scFv aL2 was purified by a one-step antigen affinity chromatography. The purified scFv aL2 was used for K_D determination by fluorescence titration (Figure 2(b) and (c)). For ampicillin, a K_D value of 1.5×10^{-6} M was obtained. Various ampicillin analogs were also used for quantitative epitope mapping by direct K_D determination of the analogs (see below). Results from inhibition studies by phage-ELISA are in good agreement with the

† http://imgt.cnusc.fr:8104/
‡ http://www.ibt.unam.mx/vir/V_mice.html

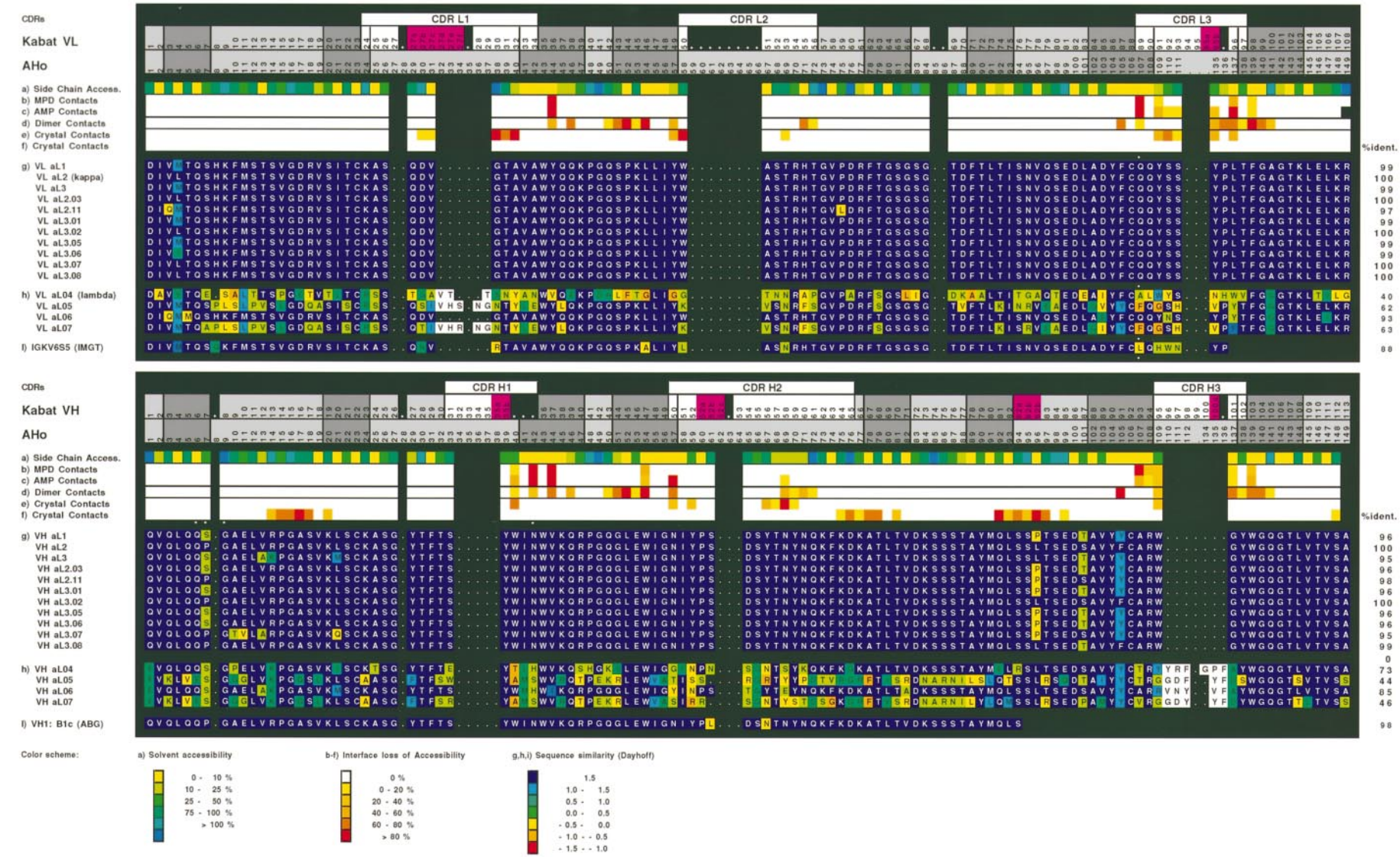

Figure 1 *(legend opposite)*

Table 1. The different crystal forms obtained with native and mutant anti-ampicillin scFv

scFv	Form	Space group	Cell (Å)	Resolution (Å)	Mol/a.u.	Ligand
aL2-$6_Q7_P10_A$ (w.t.)	1	$P4_12_12$	62.2 × 62.2 × 136.8	2.44	1	MPD
aL2-$6_Q7_P10_A$ (w.t.)	2	$C222_1$	81.2 × 93.4 × 150.9	3.00	2	None
aL2-$6_E7_P10_G$	3	$P2_12_12_1$	59.7 × 89.9 × 97.3	2.7	2	None
aL2-$6_E7_P10_G$	3	$P2_12_12_1$	59.7 × 89.9 × 97.3	2.40	2	Ampicillin
aL2-$6_E7_S10_G$	4	$P\ 4_1\ 2_1\ 2$	61.1 × 61.1 × 135.6	1.85	1	None

K_D values obtained by direct fluorescence titration of the soluble scFv (see below, Figure 6(b)). In cases where an analog might have a reduced ability to quench the tryptophan fluorescence and thus give a reduced signal in the direct fluorescence titration assay, the compound was tested for its ability to compete with ampicillin for binding and to revert the fluorescence quenching by ampicillin. The ampicillin-mediated quenching was reversed completely by the addition of β-lactamase, reflecting the inability of aL2 to bind hydrolyzed ampicillin (Figure 2(b)). When expressed in *E. coli*, the aL2 antibody was shown to mediate no detectable growth advantage in the presence of 10 μM ampicillin.

Crystal growth and overall structure of aL2 w.t.

Two crystal forms were obtained from protein solutions of the wild-type (w.t.) aL2 scFv (Table 1). The structures of aL2 form 1 and form 2 were determined at 2.4 Å and 3.0 Å resolution, respectively, with final *R*-factors and R_{free} of 17.5 % and 24.3 %, and 17.8 % and 23.2 %, respectively. In the absence of hapten, crystals of form 1 grew in the presence of 5 % (v/v) methylpentane diol (MPD) within two weeks. In the presence of 20 mM ampicillin, the same crystal form was obtained in about two months. The crystals belong to the tetragonal space group $P4_12_12$ with unit cell constants $a = b = 62.2$ Å, $c = 136.8$ Å. The volume solvent content is 49 % (v/v).[29] Crystals of form 2 grew in about 3 days from the same protein solution in the absence of MPD. The form 2 crystal belongs to the orthorhombic space group $C222_1$, with unit cell constants $a = 81.2$ Å, $b = 93.5$ Å, $c = 150.9$ Å, with two scFv per asymmetric unit. Residues not visible in the electron density map are the N-terminal FLAG tag[30] on V_L (sequence DYK), the last two V_L residues (L148 and L149, Kabat L107 and L108), the $(GGGGS)_4$ linker, the first (H1) and last (H147, Kabat H113) V_H residues and the C-terminal His tag. Twelve side-chains are poorly defined. All the residues are in allowed regions of the Ramachandran plot, with the exception of Ala L67 (L51), which shows torsion angles in the forbidden region for the majority of the V_L domain in the PDB database (164 out of 174, A. Honegger, unpublished results). Most (83.1 %) of the residues are located in the most-favored regions (PROCHECK). Form 2 has one more residue visible, at the end of the V_L domain. In both cases, the crystals have no sharp edges, they are shaped as quadratic smoothed lenses.

The V_L domain of the anti-N9-neuraminidase antibody NC41 (PDB entry 1NCA[32]) and the V_H domain of the anti-lysozyme-antibody D11.15 (PDB entry 1JHL[33]) were used to determine the aL2 structure by molecular replacement. Their C^α atoms could be superimposed on the corresponding atoms of aL2 with rms values of 1.06 Å and 0.88 Å (without the CDR3 region), indicating that the aL2 overall fold remains close to the parent structures. The complete V_H domain of D11.15 is well superimposed on aL2 with the exception of the CDR3, which is shortened by six residues in aL2. The two wild-type aL2 structures are quasi-

Figure 1. Annotated sequence alignment of anti-ampicillin scFvs. Residues are numbered according to the Kabat and the AHo unified numbering scheme.[1] (a) Relative side-chain solvent-accessibility calculated for the unliganded scFv aL2 w.t. form 2. The side-chain solvent-accessible surface of each residue was calculated as a percentage of the solvent-accessible surface the same residue would have in the context of a poly(Ala)peptide in extended conformation (program naccess (http://sjh.bi.umist.ac.uk/naccess.html)) (yellow, 0-10 %; yellow-green, 10-25 %, buried; green, 25-50 %; green-blue, 50-75 %, semi-buried; blue, 75-100 %; dark blue, >100 %, exposed). (b) and (c) MPD and ampicillin contact residues, respectively. Relative reduction of the side-chain accessible surface of each residue in the complexed scFv fragment compared to the same residue in the Fv fragment without ligand (white, 0 % reduction; yellow, 0-20 %; yellow-orange, 20-40 %; orange, 40-60 %; red-orange, 60-80 %; red, 80-100 %). (d) Dimer contact residues. (e) Crystal contact residues involved in blocking the antigen-binding side (aL2 w.t. form 1 and 2, aL2-$6_E7_S10_G$) in the molecule being blocked (Mol. 1 in Figure 4(b)). (f) Crystal contact residues involved in blocking the antigen-binding side (aL2 w.t. form 1 and 2, aL2-$6_E7_S10_G$) in the blocking molecule (Mol. 2 in Figure 4(b)). (g) Sequences of ampicillin binding scFvs from phages eluted by unspecific elution with GlyHCl pH 2.2 and by competition with ampicillin (aL1, aL2, aL3) colored by similarity to the reference sequence aL2. (h) Sequences of ampicillin-binding scFvs from phages eluted from the ampicillin surface with competition by hydrolyzed ampicillin (aL4, aL5) and by APA (aL6) colored by similarity to the reference sequence aL2. (i) Murine germline sequence closest to aL2: IGKV6S5 for the V_L Domain (IMGT, http://imgt.cines.fr:8104/textes/IMGTrepertoire/2/protein/mouse/IGK/IGKV/Mu_IGKVallgenes.html) and VH1-B1c for the V_H Domain (ABG, http://www.ibt.unam.mx/vir/Alivhmus.html#AAvh).

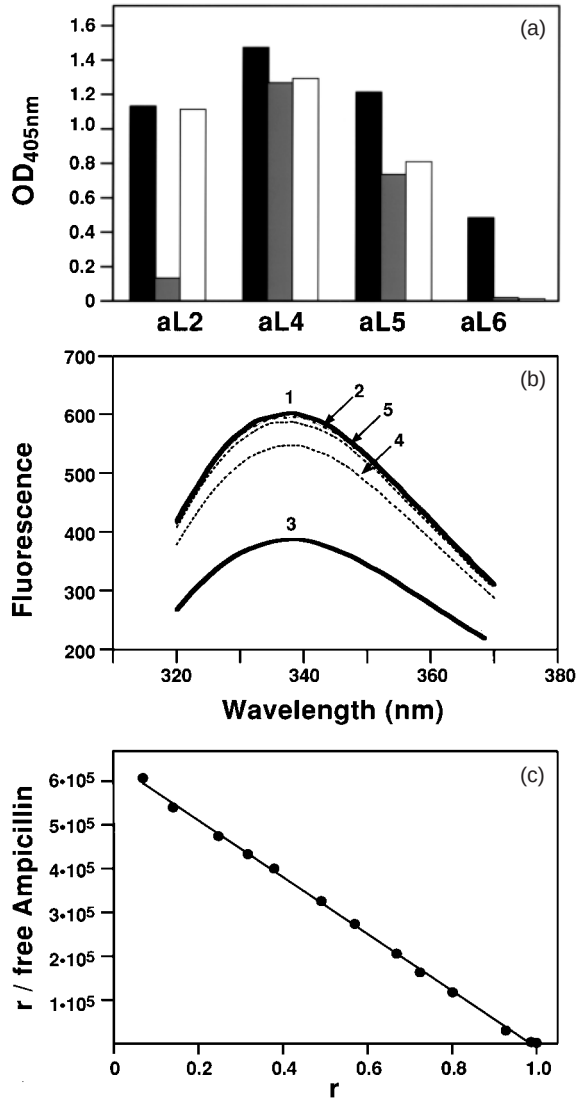

Figure 2. (a) Phage-ELISA analysis of aL2, aL4, aL5 and aL6 on transferrin-ampicillin-coated plates. The signals correspond to 10^{11} phage particles (in 100 µl). Black bars reflect specific binding. Competitive inhibition was studied by pre-incubation with 1 mM ampicillin (grey bars) and 1 mM 6-APA (white bars). (b) Change of fluorescence spectra upon Amp addition and its reversal by β-lactamase. Fluorescence titration with aL2 and ampicillin. No quenching is detectable by comparision of the initial signal (1) and the signal after addition of hydrolyzed ampicillin (2) (final concentration of 250 µM). After addition of ampicillin (final concentration of 25 µM) the signal intensity, measured after 15 seconds, is significantly lower (3). In the presence of 0.005 unit/ml β-lactamase, the signal increases again: curve (4) is measured after two minutes and curve (5) after five minutes. (c) Fluorescence titration curve evaluated according to Scatchard.[42]

identical (see Figure 4(a)). Upon superposition, a rms deviation between their C^{α} atoms of 0.46 Å is observed, which is within the range of experimental error at these resolutions. Their six CDRs are well superimposed, with the exception of Trp H109 (Kabat H95) (see Figure 4(b)), whose side-chain has a different conformation in the two structures (rms deviation of 5.9 Å). The average *B*-factors for all main-chain and side-chain atoms are 31.1 $Å^2$ and 32.9 $Å^2$, respectively. The *B*-factors of residues outside the CDR regions are very close to the mean observed for the whole Fv. All CDR main-chain atoms, with the exception of L2, exhibit *B*-factors lower than the average.

The CDR loops of aL2

The structures of five CDRs (L1, L2, L3, H1 and H2) of the antibody combining site assume a finite number of canonical conformations.[34,35] The canonical conformations of the aL2 CDRs were determined using an automated loop clustering program.[36] L1 and H2 were assigned to class 2, while the L2, L3 and H1 were assigned to class 1. The H3 loop, which does not assume any canonical structure, is particularly short in the aL2 molecule. The only other example of an antibody with an equally short CDR H3 loop is the anti-p24 (HIV-1) monoclonal antibody Cb41 (PDB entry 1CFN[37]).

Among the residues belonging to the L1 loop, Asp L30 (L28) forms a salt-bridge with the V_H domain Lys H20 (H19), and Thr L39 (L31) is tightly hydrogen bound to Gln H92 (H81) of a symmetry-related molecule. The L3 loop is stabilized by both intrasubunit (Gln L107 (L89), Gln L108 (L90) and Tyr L109 (L91)) and intersubunit hydrogen bonds and exhibits *B*-factors 30 % lower than average. The side-chain of Tyr L135 (L94) is both hydrogen bonded to the side-chain of Asn H57 (H50) and to the main-chain atoms of a symmetry-related molecule. The H2 loop is also hydrogen bonded to main-chain and side-chain atoms of a symmetry-related molecule. The side-chain atoms of Trp H109 (H95) in the H3 loop exhibit much higher *B*-factors than average (51.5 $Å^2$). This residue has two different conformations in the two crystal forms, and this directly shows the mobility that may also account for its high *B* value.

The combining site of aL2

In crystal form 1, additional electron density is observed in the combining site (Figure 3(a)). This density is quite significant, and has an elongated shape going from the bottom of the crevice to the bulk solvent. This density at the bottom of the combining site could clearly be satisfied by a MPD molecule, the precipitant in the crystallization medium, whereas the rest of the density could be filled with water molecules or disordered MPD, or both of them. Moreover, in several reported structures, ordered water molecules and alcohols have been found to replace the ligand in uncomplexed structures.[38] The MPD molecule is hydrogen bonded to Tyr L44 (L36) OH at the bottom of the binding site, and it interacts with a water molecule, part of a cluster of solvent molecules surrounding Trp H109 (H95). The final model contains one

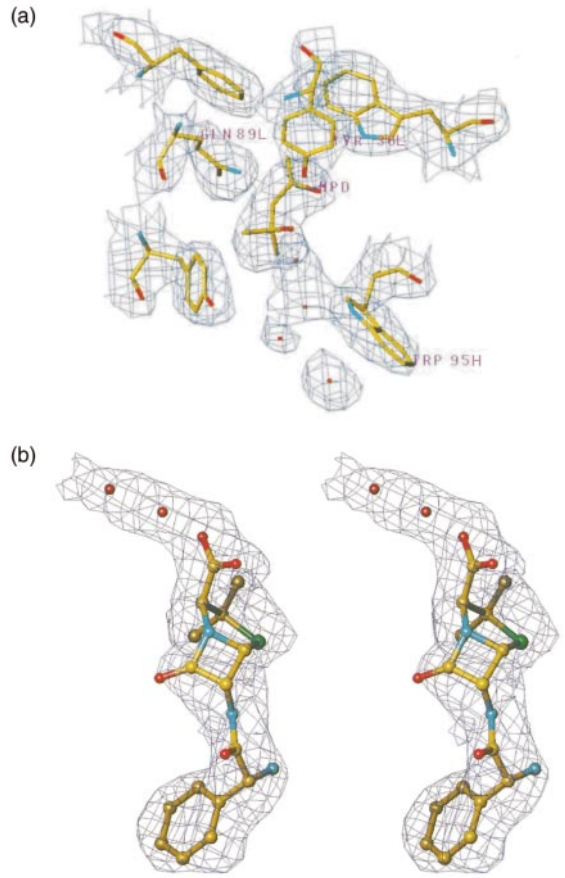

Figure 3. (a) View of MPD (in aL2 w.t. form 1) in its $2F_o - F_c$ electron density map contoured at a threshold of 0.8 sigma. (b) Stereoview of ampicillin (in aL2-$6_E7_P10_G$) in its $2F_o - F_c$ electron density map contoured at a threshold of 0.8 sigma.

MPD molecule and eight water molecules in the combining site, which resisted refinement well (average *B*-factor 47 Å^2).

In contrast, in the molecules of form 2, no electron density is visible in the combining site, which could be due to disorder of putatively bound molecules or simply to their absence. The conformational change of the side-chain of Trp H109 (H95) produces a significant change in the shape of the binding site between form 1 and form 2 (Figure 4(a) and (b)). In crystal form 2, the side-chain of Trp H109 (H95) partially fills the binding site crevice, leaving not enough space for ampicillin to bind, while in crystal form 1, the Trp H109 (H95) side-chain is turned outwards. The consequences of this simple rotation are clear in Figure 4(b). Form 2 has its combining site wide open, whereas in form 1 the entry to the binding pocket is obstructed by the Trp side-chain. Residues lining the combining site are hydrophobic or semi-polar. Hydrophobic residues comprise from bottom to top Trp H139 (H103), Ala H107 (H93), Phe L139 (L98), Tyr L109 (L91), Trp H109 (H95) and Tyr L57 (L49), Trp L58 (L50) and Trp H109 (H95) at the top. Semi-polar residues are Gln L107 (L89) and Asn H42 (H35), and Asn H57 (H50). The antigen-binding pocket contains no charged group.

Crystallization and structure of the aL2 mutants

The wild-type of aL2 never yielded crystals of the complex with ampicillin. In both crystal forms, crystal contacts obstructed the binding site, making the diffusion of ampicillin into the antigen-binding pocket impossible without disintegration of the crystal. Cocrystallization of aL2 with ampicillin failed, crystal formation was delayed for months, apparently until all ampicillin had hydrolyzed. However, in the course of a different project, several mutations were introduced into the N terminus of the heavy chain, in positions H6, H7 and H10 (H9). The packing of the crystals formed by the mutant $6_E7_P10_G$ allowed the diffusion of ampicillin into the binding pocket (see Materials and Methods).

Although the mutation of Gln H6 to Glu and of Ala H10 (H9 according to Kabat) to Gly in the mutant aL2-$6_E7_P10_G$ strongly affected the conformation of the N-terminal strand (residues H1-H10, Figure 4(a)), the residues lining the binding pocket could be superimposed almost perfectly with those of the w.t. structure, proving that the conformation of the binding site was not affected by the mutation. Only the side-chain of the tryptophan residue H109 (H95), which already varied between the two w.t. crystal structures, confirmed its flexibility by assuming yet another conformation (Figure 4(b)). A second mutant, aL2-$6_E7_S10_G$, showed the same crystal packing as the w.t. aL2 (Figure 5(b)). While the mutations affect the conformation of the N-terminal strand of the V_H domain, the superposition of the four crystal structures shows that the conformation of the antigen-binding pocket is not significantly affected (Figure 4(b)). The structure of the mutant antibody-antigen complex can therefore be used to interpret the results of the epitope mapping experiments performed with the w.t. antibody (Table 3).

The D-phenylglycine moiety of ampicillin is deeply embedded in the binding pocket, its phenyl ring making symmetric contacts to conserved residues of the V_L/V_H dimer interface: Phe L139 (L98) and Trp H139 (H103), Asn L107 (L89) and Ala H107 (H93), Tyr L44 (L36) and Val H44 (H37). Trp H109 (H95) contacts predominantly the amino group of the D-phenylglycine moiety and the amide group linking the phenylglycine moiety to the penicillic acid moiety. A hydrogen bond connects the peptide NH group of Trp H109 (H95) with the carbonyl oxygen atom of the peptide group. Leu L137 (L96), Tyr L135 (L94), Trp H40 (H33) and Asn H42 (H35) contact predominantly the penicillic acid moiety, with Asn H42 (H35) forming a hydrogen bond to the carbonyl oxygen atom of the β-lactam ring (Figures 4 and 6(a), Table 3).

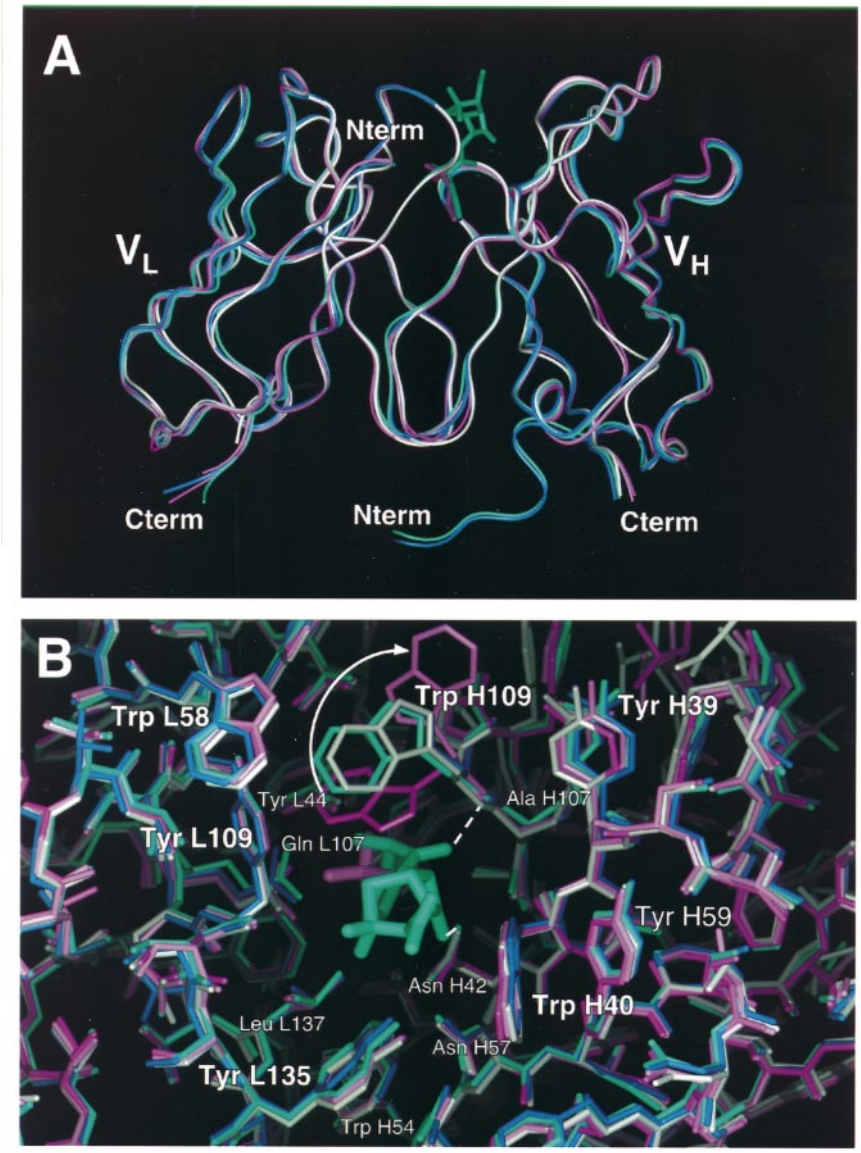

Figure 4. (a) Comparison of the overall structures. The structures of aL2 w.t forms 1 (magenta) and 2 (pink) and the two mutants aL2-$6_E7_S10_G$ (white) and aL2-$6_E7_P10_G$ (cyan, liganded structure; blue, unliganded structure) were superimposed by a least-squares fit of the C^{α} atoms of the residues forming the inner beta sheet (dimer interface) of the aL2 scFv (residues L41-L47, L51-L57, L102-L108, L138-L144, H41-H47, H51-H57, H102-H108 and H138-H144, corresponding to Kabat L33-L39, L43-L49, L84-L90, L97-L103, H35a-H40, H44-H50, H88-H94, H102-H108). (b) Close-up view of the residues contributing to the binding pocket. Hydrogen bonds between hapten and scFv are indicated by broken lines (main-chain NH of Trp H109 to O3 of ampicillin, 2.7 Å; side-chain amide NH_2 of Asn H42 to O4 of ampicillin, 2.8 Å). The distance from the amino group of Amp (N2) to the side-chain amide group of Gln L107 is too large for a hydrogen bond (3.7 Å and 3.8 Å), and the carboxylate group (O1 and O2) is exposed to the solvent.

Discussion

By a combination of intrasplenic immunization, phage display and selection for recognition of the closed-ring form, antibodies against intact ampicillin have been obtained. While aL2-related antibodies seem to dominate the immune response of mouse 4, as shown by the predominance of aL2-like scFv fragments isolated both upon unspecific elution (Gly/HCl, pH 2.2) and specific elution (competition with free ampicillin) of phages from the panning surface, scFv fragments with different specificities and selectivities could be isolated with different panning strategies.

aL2 w.t. scFvs crystallized readily in the absence of ampicillin. However, the dominant crystal contacts involved and obstructed the antigen-binding site (Figure 5(b)); in the presence of ampicillin, the onset of crystallization was delayed for two months until the antigen had hydrolyzed, and addition of ampicillin to preformed crystals led to the disintegration of the crystals. The structure of

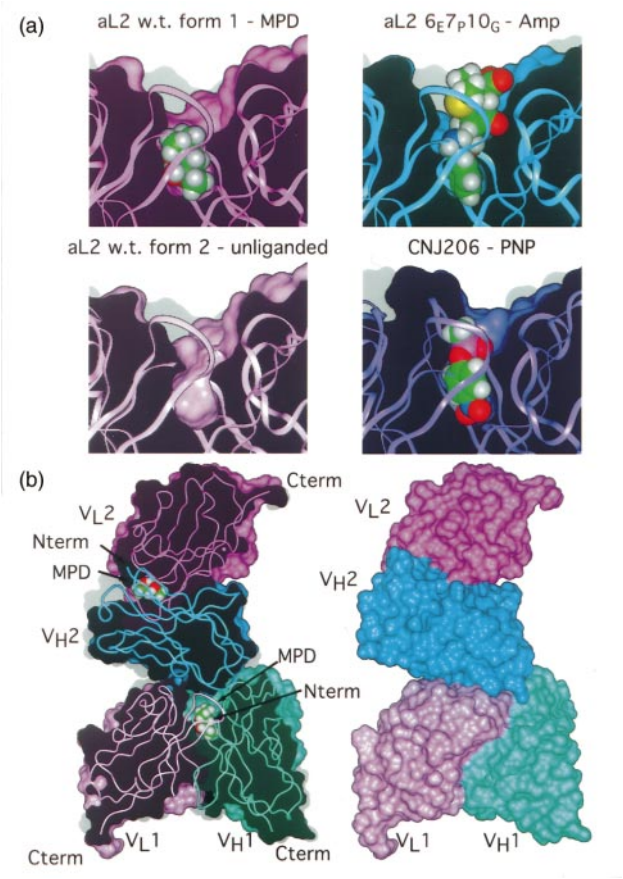

Figure 5. (a) Binding pockets of aL2 and CNJ206[40] (PDB entry 1KNO). The Conolly surface of the molecule was cut by a plane through the antigen-binding pocket. Gray shadows indicate the silhouette of the uncut surface. (b) Crystal contacts obstructing the ligand-binding pocket of aL2 wt and aL2-$6_E7_P10_G$. MPD can still be accommodated in the binding pocket, ampicillin would clash with atoms in the V_H domain of the second scFv fragment.

the unliganded scFv showed a deep, solvent-filled binding pocket (Figure 5(a)). In one of the crystal forms, the bottom of this binding pocket was occupied by a molecule of MPD, in the other form, obtained in the absence of MPD, the solvent in the pocket was disordered. The tryptophan residue H109 (H95) in the extremely short CDR H3 loop of aL2 obstructed the access to the binding pocket in one of the crystal forms, while in the other crystal form, it swung into a different conformation, leaving the access to the binding pocket open. Since all our efforts to obtain crystals of the aL2-ampicillin complex had failed, we attempted to clarify the binding mode of ampicillin by a detailed epitope-mapping scheme utilizing a wide variety of related compounds (Figure 6(b)).

Fortuitously, in the course of a different project[39] aimed at elucidating the effects of point mutations on framework 1 conformation, a mutant was obtained that crystallized in a different form. In the mutant aL2-$6_E7_P10_G$, Gln H6 had been replaced by Glu, H7 retained as Pro (this residue is Ser in 55 % of the original clones) and Ala H10 (H9) changed to Gly. This variant formed crystals in which the antigen combining site was not obstructed by crystal contacts. Ampicillin could be soaked into these crystals, and the structure of the complex could be determined. There was almost no change in the conformation of the binding pocket compared to the w.t. form, such that the complex structure could be used to interpret the binding data obtained with the w.t. aL2.

The aL2 scFv contains seven tryptophan residues. Two of these occupy highly conserved and fully buried positions (L43 (L35), H43 (H36)) in the core of the V_L and V_H domains, the other five contribute to the antigen-binding pocket. The fluorescence of the two buried Trp residues is highly quenched in the native structure of the scFv, leading to an increase of Trp fluorescence upon denaturation. Trp H54 (H47) and Trp H139 (H103) form the bottom of the binding pocket and contribute strongly to the V_H/V_L dimer interface, while Trp L58 (L50), Trp H40 (H33) and Trp H109 (H95) contribute to the rim of the binding pocket (Figure 6(a)). Thus, aL2 shows a strong tryptophan fluorescence, which is extremely sensitive to perturbation by antigen-binding. Saturating concentrations of ampicillin quenched the fluorescence intensity to 50 % of the value measured in the absence of ampicillin. Addition of minute amounts of β-lactamase completely abolished this quenching, as ampicillin was converted to the non-interacting hydrolyzed form (Figure 2(b)). This fluorescence titration allowed the direct determination of the binding constants for a wide variety of ampicillin analogs (Figure 6(b)). To verify that ampicillin fragments and analogs that did not perturb the fluorescence were indeed unable to bind, and not just unable to quench, their ability to inhibit the quenching by ampicillin competitively was determined.

Despite our efforts to bias the immunization by using different linkers to the carrier protein and to select for antibodies that predominantly recognize the penicillanic acid moiety of ampicillin, the phenyl ring of the D-phenyl glycine moiety of ampicillin (indicated in green in Figure 6(a) and (b)) is deeply embedded in the binding pocket, close to the pseudo 2-fold axis of the protein relating V_L and V_H. It is in a position similar to that of the MPD molecule in one of the unliganded structures. Its main contact residues (Trp H139 (H103), Ala H107 (H93) and Gln L107 (L89)) are highly conserved residues of the V_L/V_H dimer interface. The phenyl ring of ampicillin reaches down into the binding pocket as deeply as the nitro group of the *para*-nitrophenol hapten in the structure of the catalytic antibody CNJ206[40] (PDB entry 1KNO, Figure 5(a)). This conserved phenyl and nitrophenyl binding pocket is utilized by several different hapten-binding antibodies contained in the PDB, indicating a preferred binding mode for haptens

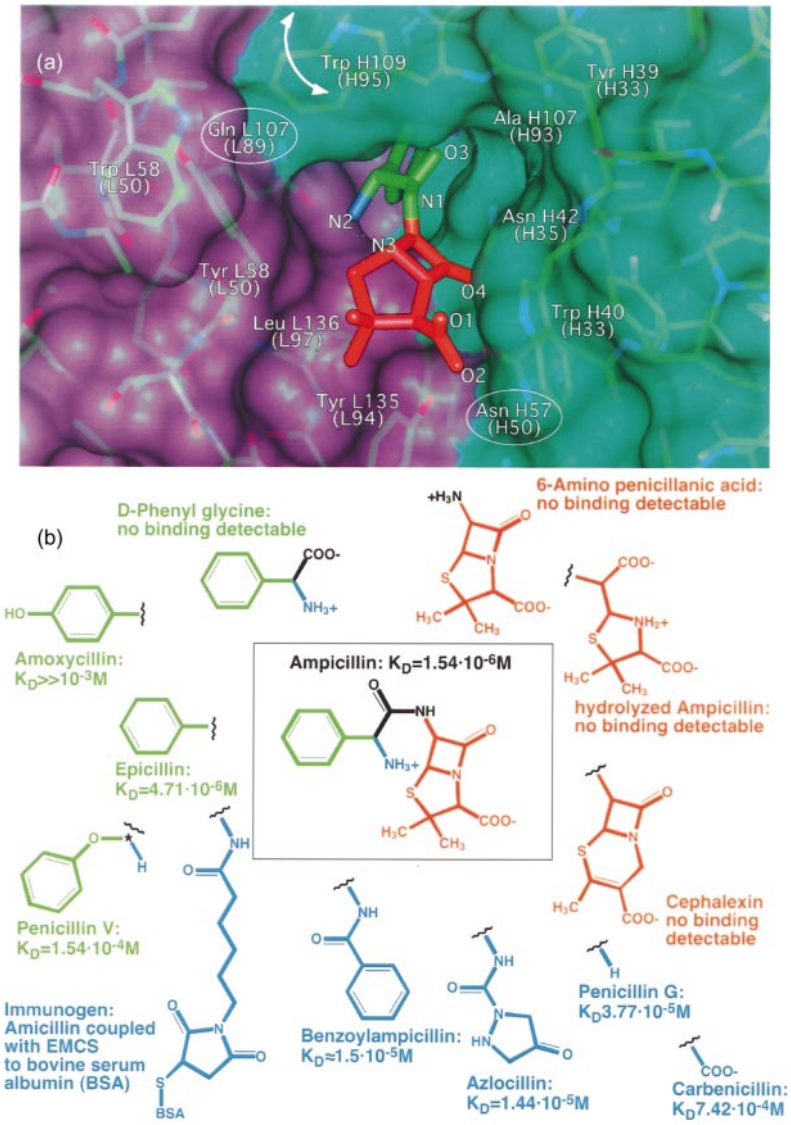

Figure 6. Epitope mapping. (a) Ampicillin in the binding pocket of aL2-$6_E7_P10_G$. (b) Ampicillin analogs with K_D values measured by fluorescence titration of the purified scFv fragment with the compounds indicated.

containing such groups (PDB entries 1AOQ, 1AJ7, 1AXS, 1D6V, 17E8, 1KEL, 1KNO, 1YEC and related antibodies).

We did not exactly obtain the desired binding mode in which the phenylglycine moiety and the linker are exposed and the penicillanic acid moiety is placed in the depth of the pocket. An antibody was generated where the amino group of the D-phenylglycine moiety (N2, indicated in blue in Figure 6), to which the linker was attached in the immunogen, is embedded fairly deeply in the pocket. However, a solvent channel to the surface remains open, which in the antibody accommodated the linker of the hapten to the carrier protein. Since we were selecting for antibodies that did not have affinity for a particular linker, and that allowed free ampicillin to displace them from the immobilized hapten, this channel does not provide optimal binding contacts to any one of the linkers used. It can be expanded further to accommodate bulkier substituents, such as the aromatic ring in benzoylampicillin, if the flexible side-chain of Trp H109 (H95) swings from the conformation seen in the liganded structure to the even more open one seen in one of the unliganded structures. The bulky groups linked as amide groups (such as in azlocillin and benzoylampicillin) to the amino nitrogen atom of ampicillin therefore reduce the binding affinity by a factor of only 10. The Gln L107 (L89) side-chain amide group is located close to the free amino group (N2) of ampicillin, which is an amide nitrogen atom in the immunogen. Deletion of this amino group (in penicillin G) leads to a 24-fold reduction of the affinity, replacement by a carboxylate group (in carbenicillin) to an almost 500-fold reduction. A mutant in which Gln L107 (H89) has been replaced by glutamate showed similar binding to ampicillin as the w.t.. However, this was determined only semi-quantitatively by phage ELISA (data not shown).

The addition of a hydroxyl group in the *para* position at the phenyl residue of ampicillin, such

as in amoxicillin (Figure 6(b)), results in reducing the binding affinity by three orders of magnitude, and an oxygen atom inserted between the C^{α} of the D-phenyl glycine moiety and the phenyl ring in penicillin V reduced the affinity by two orders of magnitude. This shows that the size of the pocket receiving the phenyl ring is limited, and that the spacing to the penam ring cannot be increased. Indeed, if the penam moiety were assumed to bind in an unchanged manner, the OH group of amoxicillin and the phenyl group of penicillin V would clash with the side-chain of Trp H139 (H103). Thus, aL2 discriminates against different acyl groups on the 6-APA backbone more than typical β-lactamases, which accept a wider variety of side-chains. The deviation from planarity in the non-aromatic ring of epicillin influences the affinity by a factor of only 3, compared to ampicillin.

The amide carbonyl group of the phenylglycine moiety (O3) accepts a hydrogen bond from the Asn H42 (H35) side-chain, while the carbonyl group of the β-lactam ring (O4) is located between Asn H42 (H35) and Asn H57 (H50), able to accept a hydrogen bond from either of them. However, Asn H42 (H35) can donate a hydrogen bond to either O3 or O4, not to both of them, depending on the conformation of this side-chain. A mutant in which Asn H57 has been replaced by Asp showed severely reduced binding, as determined by phage ELISA (data not shown). This is probably due to the loss of the hydrogen bond to O4, to unfavorable electrostatic interactions, as Asn H57 is located fairly close to the carboxylate group (O1, O2) of the aminopenicillanic acid moiety of the hapten.

At the concentrations used in the epitope mapping experiments, phenylglycine does not quench the aL2 Trp fluorescence to a measurable degree. Phenylglycine amide inhibits quenching by ampicillin to some extent, but with a complex concentration-dependence that has not been evaluated in a quantitative manner. It is possible that more than one molecule of phenylglycine can bind to the antibody.

Although 6-APA is unable to displace ampicillin at the concentrations tested, its atoms contribute significantly to the binding of ampicillin, as seen in the structure of the complex. Cephalexin, in which the five-membered thiazolidin ring of the penicillanic acid moiety has been replaced by a six-membered ring, is not recognized by aL2, nor is hydrolyzed ampicillin, in which the β-lactam ring has been opened (Figure 6(b)). In both cases, the overall conformation of the heterocyclic ring system is changed, therefore the loss of binding cannot be traced to any individual interaction.

The carboxylate group of the ampicillin (O1,O2) is quite exposed and not involved in tight interactions. Ampicillin derivatives substituted on this group have not been tested. It might be interesting to couple ampicillin to a linker through this group. aL2 could then be mutagenized and panned to select for molecules in which the solvent channel that accommodated the original linker to N2 has been filled up, yielding additional interactions and higher affinities.

The binding affinity of ampicillin to aL2 is relatively modest, with a K_D of 1.5 μM. The phage panning experiments from the same libraries using unspecific elution indicate that higher-affinity antibodies may simply not have been present in the library. Recent experiments with *in-vitro* affinity maturation of antibodies show that the competitive elution with excess hapten under the conditions utilized will not favor high-affinity affinity antibodies,[41] and in a directed evolution experiment for higher affinity, the elution strategy would have to be changed.

In conclusion, an antibody against an unstable antigen has been obtained and structurally characterized. It recognizes the desired part of the molecule. Nevertheless, this antibody, combined with knowledge of the structure of the complex, provides a promising model system for directed evolution experiments. We do believe that this antibody could provide a valuable fast assay for antibiotics.

Materials and Methods

Immunization and scFv library construction

For the preparation of the immunogen, 20 mg of BSA was dissolved in 2 ml of 8 M urea, 0.2 M Tris-HCl (pH 8.6). After addition of 4 mg of DTT and one hour incubation at 30 °C, the reduced protein was precipitated in the presence of 10 % (w/v) TCA. After centrifugation, the pellet was washed four times with water and finally dissolved in 8 M urea, 50 mM sodium phosphate (pH 7.0). In parallel, 1 ml of 25 μM ampicillin, dissolved in 50 mM sodium phosphate (pH 7), was added to 0.5 ml of a mixture of 5 mM EMCS (Fluka), 2.5 mM GMBS (Fluka) and 2.5 mM MPS (Fluka), each dissolved in tetrahydofuran (THF). After 30 minutes of incubation at 30 °C, this mixture was added to the reduced protein and after a reaction time of two hours at room temperature, the ampicillin-BSA conjugate was dialyzed for 2.5 hours at 4 °C against 5 l of PBS (20 mM sodium phosphate, 150 mM NaCl, pH 7.2).

The initial immunization of four BALB/c mice was performed by subcutaneous priming with 800 μg of AdjuPrime (Pierce) and 100 μg of ampicillin-BSA conjugate. After 16 days, 10 μg (mouse 1 and 2) or 50 μg (mouse 3 and 4) of the ampicillin-BSA conjugate was injected directly into the spleen.[27] For mouse 2, the intrasplenic injection was repeated with 30 μg of ampicillin-BSA conjugate after 37 days. Mouse 4 obtained a booster injection (250 μg) into the tail vein after 50 days. The immune response was controlled by ELISA with a transferrin-EMCS-ampicillin surface and serum (1:500 dilution).

After 43 days (mouse 2) or 54 days (mouse 4), respectively, the spleen was pressed through a sieve and suspended in 10 ml of EBSS buffer (0.4 g/l KCl, 6.8 g/l NaCl, 2.2 g/l $NaHCO_3$, 0.158 g/l $NaH_2PO_4 \cdot H_2O$, 1 g/l D-glucose) (Gibco). Connective tissue was separated by centrifugation (15 seconds at 200 ***g***) and the supernatant was transferred into a fresh tube and centrifuged for seven minutes at 250 ***g***. The cells were resuspended for mRNA preparation in 2 ml of extraction buffer (Pharma-

cia QuickPrep mRNA Purification Kit). For construction of an scFv antibody library, the reverse transcribed mRNA was PCR amplified by using specific primers, designed to represent the murine immune response within the phage display vector pAK100.[25]

Phage panning

For selection of antigen-binding phages, immunotubes (Nunc, Maxisorp) were coated overnight at 4 °C with 4 ml of transferrin-EMCS-ampicillin (100 μg/ml) in a 1:1 mixture of PBS and urea-sodium phosphate (8 M urea, 50 mM sodium phosphate, pH 7.0). After blocking with 4 % (w/v) dried skimmed milk powder in PBS for two hours at room temperature, 10^{11} phage particles in 4 ml of PBS containing 2 % milk were added and incubated for two hours with rocking at room temperature. Tubes were then washed 15 times with PBS/0.1 % (v/v) Tween and 15 times with PBS. Bound phages were eluted by incubation for ten minutes with either 800 μl of 0.1 M glycine/HCl (pH 2.2) or 1 ml of soluble antigen (1 mM ampicillin, 1 mM 6-APA or 1 mM hydrolyzed ampicillin). Hydrolyzed ampicillin was prepared freshly by incubation of 1 ml of 10 mM ampicillin with two units of RTEM β-lactamase. Reinfection of *E. coli* XL1-Blue cells, phage propagation and binding analysis by phage ELISA were performed as described.[25]

Purification of aL2

For soluble expression, the scFv-aL2 was cloned into pAK300.[25] HCDC cultivation with glucose feeding under limited growth conditions was performed at 26 °C by using *E. coli* RV308.[24] The cells were harvested by centrifugation after four hours induction with 1 mM IPTG (final $A_{550\ nm} = 46$). Cells were resuspended in BBS/1 M NaCl (pH 7.5) and disrupted twice in a French press. For purification, an affinity column was used for which 10 mM ampicillin was coupled to Affi-Gel 10 (Biorad). After loading, washing steps with BBS/1 M NaCl (pH 7.5), BBS/150 mM NaCl (pH 7.5) and 10 mM Hepes (pH 7.0) were performed. It was essential to carry out the washing step with 10 mM Hepes (pH 7.0), by which the contaminating chloramphenicol acetyltransferase (CAT), which fortuitously also binds to the affinity column, can be eluted selectively. After an additional high-salt washing step with BBS/1 M NaCl (pH 7.5) the antibody fragment was eluted with 5 mM ampicillin in the same buffer. Three dialysis steps were performed against 10 mM Tris/HCl (pH 7.0), 10 mM NaCl, 0.002 % (w/v) NaN_3.

Determination of the Hapten-binding constants

Fluorescence emission spectra of 10^{-7} M scFv aL2 and antigen (freshly prepared solutions of ampicillin, amoxicillin, 6-APA, azlocillin, benzoylampicillin, cephalexin, carbenicillin, D-phenylglycine, epicillin, hydrolyzed ampicillin, penicillin G and penicillin V) were measured at 20 °C in HBS buffer (10 mM Hepes (pH 7.4), 150 mM NaCl, 3.4 mM EDTA, 0.005 % (v/v) surfactant P-20) (Pharmacia Biosensor) with a Shimadzu spectrofluorimeter (RF-5000) using an excitation wavelength of 280 nm. For the K_D determination, the emission was monitored at 342 nm and evaluated according to Scatchard.[42]

Crystallization and structure determination of w.t. aL2 and mutant $6_E7_P10_G$

Crystallization experiments used the hanging drop technique with local and commercially available sparse-matrix,[43] as well as with an antibody screen designed by Stura *et al*.[44] The Fv aL2-wt crystallized at 20 °C in two crystal forms (Table 1). Crystals of form 1 were obtained from a 16 mg/ml protein solution using 1.75 M ammonium sulfate, 50 mM phosphate buffer (pH 6.5) and 5 % (v/v) MPD as precipitant. Crystal growth took about two months and crystals belong to the space group $P4_12_12$; they diffract to 2.44 Å resolution. The same protein solution was used to grow crystals form 2, using 1.75 M ammonium sulfate, 0.05 M phosphate (pH 5.5) and 5 % (v/v) isopropanol. Crystals grew in about three days, diffract up to 3.0 Å and belong to the orthorhombic space group $C222_1$.

Crystals of unliganded mutant Fv aL2-$6_E7_P10_G$ appeared in one week, starting from a protein solution at 3 mg/ml and using a well solution of 26 % (w/v) polyethylene glycol 2000 monomethyl-ether, 200 mM ammonium sulfate and 100 mM sodium acetate (pH 5.0). Crystals of the mutant complexed with the hapten were obtained by repetitive incubation of the unliganded mutant crystals into a fresh preparation of the mother liquor containing 33 mM ampicillin. Crystallographic parameters are summarized in Table 2.

Data sets were collected using a Mar-300 imaging plate detector system mounted on a Rigaku RU 200 rotating anode, operating at 40 kV and 80 mA with a graphite monochromated CuKα radiation. Data were collected at room temperature and up to 3.0 Å for crystal form 1 and up to 2.44 Å for crystals form 2 of the Fv aL2-wt. Data of the mutant Fv aL2-$6_E7_P10_G$ were colleted using cryo-protected crystals (14 % (v/v) glycerol). The data were indexed and intergrated using DENZO,[45] and scaled and merged using SCALEPACK and CCP4[46] for the w.t. and the mutant, respectively (Table 2).

The structure of crystal form 2 was determined by molecular replacement. Searches were run using the program AMoRe.[47] The starting model of the V_L domain was from the structure of the anti-N9-neuraminidase antibody NC41,[32] with which it shares 84.3 % of sequence identity. The V_H domain of aL2 was modeled using the V_L of the anti-lysozyme antibody D11.15[33] as a template with 89.7 % sequence identity with the aL2 V_H sequence. The rotation and translation functions were calculated over a resolution range of 8-3.5 Å with a Patterson integration radius of 20 Å. The molecular replacement solution, which included two protein molecules per asymmetric unit, gave a correlation coefficient of 38.5 % and an *R*-factor of 41.6 %. This structure was refined with the simulated annealing and conjugate-gradient X-PLOR version 3.1[48] strictly restraining the non-crystallographic symmetry all along the refinement. After each refinement cycle, a new map was calculated and the model rebuilt using the molecular modeling program TURBO-FRODO.[49]

The model obtained from the refinement of crystal form 2 was correctly placed in the cell of the crystal form 1 (one molecule per asymmetric unit), running again the program AMoRe under the same conditions. The resulting correlation coefficient was 79 % and the *R*-factor was 26.6 %. The structure of crystal form 1 was refined with X-PLOR following the same protocol used for crystal form 2. The R_{free} using 5 % of the data was monitored throughout the refinement. Final refinement data are summarized in Table 2.

Table 2. Data collection and final refinement statistics

	aL2-wt $6_Q7_P10_A$ form 1-free	aL2-wt $6_Q7_P10_A$ form 2-free	aL2-mutant $6_E7_P10_G$ form 3-free	aL2-mutant $6_E7_P10_G$ form 3-complex
Data collection				
V_m (Å^3/Da)	2.43	2.63	2.40	2.40
Data resolution (Å)	2.44	3.00	2.75	2.40
Observations	41,058	59,922	81,293	93,952
Unique	9809	11,762	14,189	20,445
Completeness (%)[a]	89.2/71.7	86.1/68.1	97.5/90.7	98.0/82.8
$I/\sigma[I]$[a]	11.0/2.5	7.0/2.0	8.0/2.0	10.0/3.0
Refinement				
Reflections	9323	10,114	13,978	19,137
Resolution (Å)	15-2.44	15-3.0	13-2.75	13-2.40
R-factor/*R*-free (%)	17.5/24.3	17.8/23.2	17.7/25.7	20.5/27.7
Atoms	2032	4086	3400	3400
Solvent atoms	78	26	110	298
B-factors (Å^2)				
Main-chains	31.10	24.66	31.3	20.88
Side-chains	32.88	27.64	35.0	23.82
Solvent	49.11	27.92	34.5	29.53
rms deviations				
Bonds (Å)	0.008	0.007	0.010	0.011
Angles (deg.)	1.811	1.685	1.60	1.58
Improper (deg.)	1.213	1.209	0.90	1.16

[a] Overall/last shell.

The Fv-aL2-$6_E7_P10_G$ mutant structure was determined using the program AMoRE, with the 2.44 Å native structure as the search model. The initial rigid-body solution gave a correlation cofficient of 47% and an *R*-factor of 45%. The structure was refined over successive rounds using the program CNS version 0.5,[48] with re-building using the program TURBO-FRODO. The N terminus of the heavy chain, residues H1-H10, was built into omit maps. The electron density was of excellent quality for residues L1 to L146 (L105) of the light chain and H1 to H147 (H111) of the heavy chain present in the model. Two sulfate anions, the ampicillin moiety and 298 water molecules were added to the model. The final model was refined to an *R*-factor of 23% and an R_{free} of 28% (Table 2). All residues, but two (Ala L67 (L51) from each monomer), are located in the most favored and additional allowed regions of the Ramachandran plot.[31] Ala L67 (L51) forms part of a classic γ-turn, which explains the unfavourable phi-psi values. The overall *B*-value is 22.3 Å^2 (20.9 Å^2 and 23.8 Å^2 for main-chain and side-chain protein atoms, repectively); no water molecule has a *B*-value greater than 50 Å^2. Clear electron density, consistent with the chemical structure of ampicillin, was observed in the binding site of one of the two Fv in the asymmetric unit.

Table 3. The scFv surfaces buried by ampicillin and the shortest contacts observed (the ampicillin atom involved in the contact is given in parentheses; see Figure 6) and of the hydrogen bonds between ampicillin and the scFv

CDR	Residues	Surface (Å^2)	Distance (Å)
L1	Tyr L44 (L36)	7	3.97 (N2)
L3	Gln L107 (89L89)	13	3.06 (C8)
	Tyr L109 (L91)	21	4.17 (C1)
	Tyr L135 (L94)	25	3.46 (C16)
	Leu L137 (L96)	18	3.67 (C7)
	Phe L139 (L98)	3	3.84 (C9)
Total L3		80	
H1	Trp H40 (H33)	43	3.50 (C15)
	Asn H42 (H35)	27	2.85 (O4)
	Val H44 (H37)	2	3.94 (C9)
Total H1		52	
H3	Ala H107 (H93)	6	3.59 (C10)
	Arg H108 (H94)	2	3.40 (O3)
	Trp H109 (H95)	44	3.12 (C4)
	Trp H139 (H103)	8	3.41 (C10)
Total H3		61	
CDR	H-bond donor	H-bond acceptor	Distance (Å)
H2	Asn H42 (H35) HND	Amp O4	2.85
H3	Trp H109 (H95) NH	Amp O3	2.72

X-ray structure of aL2 mutant $6_E7_S10_G$

This mutant was crystallized in ammonium sulfate. The crystals belong to the space group $P4_12_12$ with lattice constants $a = 61.1$ Å, $b = 61.1$ Å, $c = 135.6$ Å, $\alpha = \beta = \gamma = 90°$. An asymmetric unit contains one scFv, according to a solvent content of 47% (v/v).[29] They diffract at 1.8 Å resolution.[39]

Residue numbering

Residues are numbered according to the unified numbering scheme introduced in the accompanying manuscript[1]. In contrast to the Kabat numbering scheme, this numbering scheme gives the same residue number, distinguished by the chain label, to structurally equivalent residues in V_L and V_H domains.

Protein Data Bank accession numbers

The aL2 scFv structures have been deposited in the RCSB Protein Data Bank (http://www.rcsb.org/), entries 1I3G (aL2 w.t. form 1), 1H8N (aL2-$6_E7_S10_G$), 1H8O (aL2-$6_E7_P10_G$ unliganded) and 1H8S (aL2-$6_E7_P10_G$-ampicillin complex).

Acknowledgments

We thank Drs Martin Bachmann, Beat Kunz, Hans Hengartner and Rolf Zinkernagel for technical advice and/or expert assistance to immunization of mice. For fermentation of the aL2 wild-type antibody we thank the group of Dr Dieter Riesenberg for their helpful contributions. This work was supported by a grant from the Schweizerische Nationalfonds 3100-046624, the European Community BIO2-CT92-0367 and the CNRS.

References

1. Honegger, A. & Plückthun, A. (2001). Yet another numbering scheme for immunoglobulin variable domains: an automatic modeling and analysis tool. *J. Mol. Biol.* **309**, 657-670.
2. Matsuhashi, M. (1994). Utilization of lipid-linked precursors and the formation of peptidoglycan in the process of cell growth and division: membrane enzymes involved in the final steps of peptidoglycan synthesis and the mechanism of their regulation. In *Bacterial Cell Wall* (Ghuysen, J.-M. & Hakenbeck, R., eds), vol. 27, pp. 55-71, Elsevier Science Publisher B. V., Amsterdam.
3. EEC, (1990). *Official Journal of the European Communities, Commission Regulation (EEC)*, no. 2377/90 **(1990) L 224**, 1-8.
4. Yerian, T. D., Christian, G. D. & Ruzicka, J. (1988). Flow injection analysis as a diagnostic tool for development and testing of a penicillin sensor. *Anal. Chem.* **60**, 1250-1256.
5. Charm, S. E. & Chi, R. (1988). Microbial receptor assay for rapid detection and identification of seven families of antimicrobial drugs in milk: collaborative study. *J. Assoc. Off. Anal. Chem.* **71**, 304-316.
6. Aerts, M. M., Hogenboom, A. C. & Brinkman, U. A. (1995). Analytical strategies for the screening of veterinary drugs and their residues in edible products. *J. Chromatog. sect. B,* **667**, 1-40.
7. Usleber, E., Litz, S. & Märtlbauer, E. (1998). Production and characterization of group-specific antibodies against penicillin antibiotics. *Food Agric. Immunol.* **10**, 317-324.
8. Dietrich, R., Usleber, E. & Märtlbauer, E. (1998). The potential of monoclonal antibodies against ampicillin for the preparation of a multi-immunoaffinity chromatography for penicillins. *Analyst,* **123**, 2749-2754.
9. Smith, G. P. & Scott, J. K. (1993). Libraries of peptides and proteins displayed on filamentous phage. *Methods Enzymol.* **217**, 228-257.
10. Hanes, J. & Plückthun, A. (1997). *In vitro* selection and evolution of functional proteins by using ribosome display. *Proc. Natl Acad. Sci. USA,* **94**, 4937-4942.
11. Georgiou, G., Stathopoulos, C., Daugherty, P. S., Nayak, A. R., Iverson, B. L. & Curtiss, R., III (1997). Display of heterologous proteins on the surface of microorganisms: from the screening of combinatorial libraries to live recombinant vaccines. *Nature Biotechnol.* **15**, 29-34.
12. Kieke, M. C., Cho, B. K., Boder, E. T., Kranz, D. M. & Wittrup, K. D. (1997). Isolation of anti-T cell receptor scFv mutants by yeast surface display. *Protein Eng.* **10**, 1303-1310.
13. Winter, G., Griffiths, A. D., Hawkins, R. E. & Hoogenboom, H. R. (1994). Making antibodies by phage display technology. *Annu. Rev. Immunol.* **12**, 433-455.
14. Vaughan, T. J., Williams, A. J., Pritchard, K., Osbourn, J. K., Pope, A. R., Earnshaw, J. C., McCafferty, J., Hodits, R. A., Wilton, J. & Johnson, K. S. (1996). Human antibodies with sub-nanomolar affinities isolated from a large non-immunized phage display library. *Nature Biotechnol.* **14**, 309-314.
15. Griffiths, A. D. & Duncan, A. R. (1998). Strategies for selection of antibodies by phage display. *Curr. Opin. Biotechnol.* **9**, 102-108.
16. Knappik, A., Ge, L., Honegger, A., Pack, P., Fischer, M., Wellnhofer, G., Hoess, A., Wölle, J., Plückthun, A. & Virnekäs, B. (2000). Fully synthetic human combinatorial antibody libraries (HuCAL) based on modular consensus frameworks and CDRs randomized with trinucleotides. *J. Mol. Biol.* **296**, 57-86.
17. Low, N. M., Holliger, P. H. & Winter, G. (1996). Mimicking somatic hypermutation: affinity maturation of antibodies displayed on bacteriophage using a bacterial mutator strain. *J. Mol. Biol.* **260**, 359-368.
18. Schier, R. & Marks, J. D. (1996). Efficient in vitro affinity maturation of phage antibodies using BIAcore guided selections. *Hum. Antibodies Hybridomas,* **7**, 97-105.
19. Hanes, J., Jermutus, L., Weber-Bornhauser, S., Bosshard, H. R. & Plückthun, A. (1998). Ribosome display efficiently selects and evolves high-affinity antibodies *in vitro* from immune libraries. *Proc. Natl Acad. Sci. USA,* **95**, 14130-14135.
20. Ohlin, M., Owman, H., Mach, M. & Borrebaeck, C. A. (1996). Light chain shuffling of a high affinity antibody results in a drift in epitope recognition. *Mol. Immunol.* **33**, 47-56.
21. Parsons, H. L., Earnshaw, J. C., Wilton, J., Johnson, K. S., Schueler, P. A., Mahoney, W. & McCafferty, J. (1996). Directing phage selections towards specific epitopes. *Protein Eng.* **9**, 1043-1049.
22. Martineau, P. & Betton, J. M. (1999). *In vitro* folding and thermodynamic stability of an antibody frag-

ment selected *in vivo* for high expression levels in *Escherichia coli* cytoplasm. *J. Mol. Biol.* **292**, 921-929.
23. Wörn, A. & Plückthun, A. (1999). Different equilibrium stability behavior of scFv fragments: identification, classification, and improvement by protein engineering. *Biochemistry,* **38**, 8739-8750.
24. Plückthun, A., Krebber, A., Krebber, C., Horn, U., Knüpfer, U., Wenderoth, R., Nieba, L., Proba, K. & Riesenberg, D. (1996). Producing antibodies in *Escherichia coli*: from PCR to fermentation. In *Antibody Engineering: A Practical Approach* (McCafferty, J. & Hoogenboom, H. R., eds), pp. 203-252, IRL Press, Oxford.
25. Krebber, A., Bornhauser, S., Burmester, J., Honegger, A., Willuda, J., Bosshard, H. R. & Plückthun, A. (1997). Reliable cloning of functional antibody variable domains from hybridomas and spleen cell repertoires employing a reengineered phage display system. *J. Immunol. Methods,* **201**, 35-55.
26. Page, M. I. (1987). The mechanisms of reactions of β-lactam antibiotics. In *Advances in Physical Organic Chemistry*, vol. 23, pp. 165-270, Academic Press Inc., London.
27. Nilsson, B. O. & Larsson, A. (1990). Intrasplenic immunization with minute amounts of antigen. *Immunol. Today,* **11**, 10-12.
28. Burmester, J. & Plückthun, A. (2001). Construction of scFv fragments from hybridoma or spleen cells by PCR assembly. In *Antibody Engineering* (Kontermann, R. & Dübel, S., eds), pp. 19-40, Springer Verlag, Heidelberg.
29. Matthews, B. W. (1968). Solvent content of protein crystals. *J. Mol. Biol.* **33**, 491-497.
30. Knappik, A. & Plückthun, A. (1994). An improved affinity tag based on the FLAG peptide for the detection and purification of recombinant antibody fragments. *Biotechniques,* **17**, 754-761.
31. Laskowski, R., MacArthur, M., Moss, D. & Thornton, J. M. (1993). PROCHECK: a program to check the stereochemical quality of protein structures. *J. Appl. Crystallog.* **26**, 91-97.
32. Tulip, W. R., Varghese, J. N., Laver, W. G., Webster, R. G. & Colman, P. M. (1992). Refined crystal structure of the influenza virus N9 neuraminidase-NC41 Fab complex. *J. Mol. Biol.* **227**, 122-148.
33. Chitarra, V., Alzari, P. M., Bentley, G. A., Bhat, T. N., Eisele, J. L., Houdusse, A., Lescar, J., Souchon, H. & Poljak, R. J. (1993). Three-dimensional structure of a heteroclitic antigen-antibody cross-reaction complex. *Proc. Natl Acad. Sci. USA,* **90**, 7711-7715.
34. Chothia, C., Lesk, A. M., Gherardi, E., Tomlinson, I. M., Walter, G., Marks, J. D., Llewelyn, M. B. & Winter, G. (1992). Structural repertoire of the human V_H segments. *J. Mol. Biol.* **227**, 799-817.
35. Chothia, C., Lesk, A. M., Tramontano, A., Levitt, M., Smith-Gill, S. J., Air, G., Sheriff, S., Padlan, E. A., Davies, D., Tulip, W. R., Colman, P. M., Spinelli, S., Alzari, P. M. & Poljak, R. J. (1989). Conformations of immunoglobulin hypervariable regions. *Nature,* **342**, 877-883.
36. Martin, A. C. & Thornton, J. M. (1996). Structural families in loops of homologous proteins: automatic classification, modelling and application to antibodies. *J. Mol. Biol.* **263**, 800-815.
37. Keitel, T., Kramer, A., Wessner, H., Scholz, C., Schneider-Mergener, J. & Höhne, W. (1997). Crystallographic analysis of anti-p24 (HIV-1) monoclonal antibody cross-reactivity and polyspecificity. *Cell,* **91**, 811-820.
38. Mattos, C. & Ringe, D. (1996). Locating and characterizing binding sites on proteins. *Nature Biotechnol.* **14**, 595-599.
39. Jung, S., Spinelli, S., Schimmele, B., Honegger, A., Pugliese, L., Cambillau, C. & Plückthun, A. (2001). The importance of framework residues H6, H7 and H10 in antibody heavy chains: experimental evidence for a new structural subclassification of antibody V_H domain. *J. Mol. Biol.* **00**, 000-.
40. Charbonnier, J., Carpenter, E., Gigant, B., Golinelli-Pimpaneau, B., Eshhar, Z., Green, B. & Knossow, M. (1995). Crystal structure of the complex of a catalytic antibody Fab fragment with a transition state analog: structural similarities in esterase-like catalytic antibodies. *Proc. Natl Acad. Sci. USA,* **92**, 11721-11725.
41. Jermutus, L., Honegger, A., Schwesinger, F., Hanes, J. & Plückthun, A. (2001). Tailoring *in vitro* evolution for protein affinity or stability. *Proc. Natl Acad. Sci. USA,* **98**, 75-80.
42. Scatchard, G. (1949). The attraction of proteins for small molecules and ions. *Ann. NY. Acad. Sci.* **51**, 660-672.
43. Jancarik, J. & Kim, S. H. (1991). Sparse matrix sampling: a screening method for crystallization of proteins. *J. Appl. Crystallog.* **24**, 409-410.
44. Stura, E. A., Nemerow, G. R. & Wilson, I. A. (1992). Strategies in the crystallization of glycoproteins and protein complexes. *J. Crystal Growth,* **122**, 273-285.
45. Otwinovski, Z. (1993). DENZO: oscillation data and reducing program. In *Data Collection and Processing* (Sawyer, L., Isaacs, N. W. & Bailey, S., eds), pp. 56-63, DLSCI/R34 Daresbury Laboratory, Warrington, England.
46. CCP4, Number 4 Collaborative Computational Project (1994). The CCP4 suite: programs for protein crystallography. *Acta Crystallog. sect. D,* **50**, 760-763 .
47. Navaza, J. (1994). AMoRe: an automated package for molecular replacement. *Acta Crystallog. sect. A,* **50**, 157-163.
48. Brünger, A. T., Adams, P. D., Clore, G. M., DeLano, W. L., Gros, P., Grosse-Kunstleve, R. W., Jiang, J. S., Kuszewski, J., Nilges, M., Pannu, N. S., Read, R. J., Rice, L. M., Simonson, T. & Warren, G. L. (1998). Crystallography & NMR system: a new software suite for macromolecular structure determination. *Acta Crystallog. sect. D,* **54**, 905-921.
49. Roussel, A. & Cambillau, C. (1991). The TURBO-FRODO graphics package. In *Silicon Graphics Geometry Partners Directory (Silicon Graphics)*, p. 81, Mountain View, USA.

Edited by I. Wilson

(Received 4 December 2000; received in revised form 28 March 2001; accepted 29 March 2001)